Classical Monte Carlo algorithm for simulation of a pseudospin model for cuprates

V A Ulitko¹, Yu D Panov¹, A S Moskvin¹

 $^{1} \rm Institute$ of Natural Sciences and Mathematics, Ural Federal University, 19 Mira str., Ekaterinburg , Russia

E-mail: vasiliy.ulitko@urfu.ru

Abstract. A classical Monte Carlo algorithm based on the quasi-classical approximation is applied to the pseudospin Hamiltonian of the model cuprate. The model takes into account both local and non-local correlations, Heisenberg spin-exchange interaction, single-particle and correlated two-particle transfer. We define the state selection rule that gives both the uniform distribution of states in the phase space and the doped charge conservation. The simulation results show a qualitative agreement of a phase diagrams with the experimental ones.

1. Introduction

The phase diagram of doped HTSC cuprates is the subject of active experimental [1, 2] and theoretical research, despite the huge amount of work on this topic to date. A striking feature of the phase diagram of HTSC cuprates is the competition and coexistence of antiferromagnetic, superconducting, and charge orderings [3], manifested in pseudogap phase, strange metal phase, a variety of static and dynamic fluctuations. The studies are complicated by the presence of heterogeneity due to dopants or non-isovalent substitution, as well as to the internal electronic tendency to heterogeneity [4]. Phase separation may be the cause of simultaneous detection of the preformed pairs and BEC superconductivity in cuprates [2], a number of experimental observations of the typical Fermi liquid behavior, at least in overdoped cuprates. For models describing such complex multiphase states, the calculation of phase diagrams within the exact schemes is obstructed due to the absence of one leading parameter, and therefore, to obtain physically reliable results it is natural to use straightforward techniques, such as the mean field approximation and the classical Monte Carlo method.

Previously, we developed a minimal model of the HTSC cuprates [5, 6], where the CuO_2 planes are considered as lattices of centers, which are the main element of the crystal and electronic structure of cuprates. In this model, on-site Hilbert space is formed by three effective valence states of the CuO_4 cluster: $[CuO_4]^{7-}$, $[CuO_4]^{6-}$, and $[CuO_4]^{5-}$. The necessity to consider these valence states of CuO_4 center on an equal basis is related to the strong relaxation effects of the electron lattice in cuprates [7, 8]. The valence states of CuO_4 center have different spin states: s = 1/2 for the $[CuO_4]^{6-}$ center and s = 0 for the $[CuO_4]^{7-}$ and $[CuO_4]^{5-}$, respectively, and different symmetry of the orbital states: B_{1g} for the ground states of the $[CuO_4]^{6-}$ center, A_{1g} for the $[CuO_4]^{7-}$ center, and the Zhang-Rice A_{1g} or more complicated low-lying non-Zhang-Rice states for the $[CuO_4]^{5-}$ center. For these many-electron states with strong p-d covalence and strong intra-center correlations, electrons cannot be described within

conventional (quasi)particle approach that addresses the $[CuO_4]^{7-,6-,5-}$ centers within the onsite hole representation $|n\rangle$, n=0,1,2, respectively. We make use of a real space on-site S=1 pseudospin formalism to describe the charge triplets instead of conventional quasiparticle k-momentum description. The pseudospin approach is used for the strongly correlated electron systems [9, 10] and for the superconductivity [11] of cuprates for a long time. In our model, the effective pseudospin Hamiltonian takes into account both local and nonlocal correlations, single and two-particle transport, as well as Heisenberg spin-exchange interaction. Earlier, we investigated a simplified static version of the spin-pseudospin model, for which phase diagrams of the ground state and at a finite temperature were constructed, both analytically, in the mean field approximation [12], and as a result of Monte Carlo simulations [13]. The use of pseudospin formalism provides opportunities for numerical modeling using the well-developed classical Monte Carlo (MC) method, the construction of phase diagrams and the study of the features of the thermodynamic properties of the system. A similar effective S=1 spin-charge model for cuprates and its MC implementation were considered in papers [14, 15].

We organize the article as follows. In Section 2, we present the pseudospin formalism and the effective spin-pseudospin Hamiltonian of the model and introduce quasi-classical approximation. In Section 3, we formulate the state selection algorithm and explore the features of the probability distribution. The results of classical MC simulations of our model and their discussion are presented in Section 4.

2. Model

We develop a pseudospin model of cuprates [5, 6] where the CuO_2 planes are considered as lattices of CuO_4 clusters, which are the main element of the crystal and electronic structure of cuprates. The on-site Hilbert space is formed by 4 states. The effective valence states of the cluster, $[\text{CuO}_4]^{7-}$, $[\text{CuO}_4]^{6-}$, and $[\text{CuO}_4]^{5-}$, have different spin states: formally one-hole $[\text{CuO}_4]^{6-}$ center is the s=1/2 doublet, while the $[\text{CuO}_4]^{7-}$ and $[\text{CuO}_4]^{5-}$ centers are the spin singlets. As a result, the basis $|SM;s\mu\rangle$ on a given site is the quartet of states $\{|11;00\rangle, |10; \frac{1}{2}\frac{1}{2}\rangle, |10; \frac{1}{2}, -\frac{1}{2}\rangle, |1, -1;00\rangle\}$.

The effective pseudospin Hamiltonian of the model cuprate

$$\mathcal{H} = \mathcal{H}_{pot} + \mathcal{H}_{kin}^{(1)} + \mathcal{H}_{kin}^{(2)} + \mathcal{H}_{ex} \tag{1}$$

takes into account both local and nonlocal charge correlations

$$\mathcal{H}_{pot} = \sum_{i} \left(\Delta S_{zi}^{2} - \mu S_{zi} \right) + V \sum_{\langle ij \rangle} S_{zi} S_{zj}, \tag{2}$$

the three types of the correlated single-particle transport

$$\mathcal{H}_{kin}^{(1)} = -\sum_{\langle ij\rangle\nu} \left[t_p P_{i+}^{\nu} P_{j-}^{\nu} + t_n N_{i+}^{\nu} N_{j-}^{\nu} + \frac{t_{pn}}{2} \left(P_{i+}^{\nu} N_{j-}^{\nu} + N_{i+}^{\nu} P_{j-}^{\nu} \right) + h.c. \right], \tag{3}$$

the two-particle transport

$$\mathcal{H}_{kin}^{(2)} = -t_b \sum_{\langle ij \rangle} \left(S_{i+}^2 S_{j-}^2 + S_{j+}^2 S_{i-}^2 \right), \tag{4}$$

and finally, the antiferromagnetic Heisenberg spin-exchange interaction for the CuO_4^{6-} centers,

$$\mathcal{H}_{ex} = Js^2 \sum_{\langle ij \rangle} \sigma_i \sigma_j, \tag{5}$$

where $\sigma = P_0 \, {\rm s}/{\rm s}$ operators take into account the on-site spin density $P_0 = 1 - S_z^2$, and ${\rm s}$ is the spin s = 1/2 operator. The pseudospin operator S_z in (2) gives the value of charge counted from "parent" $[{\rm CuO_4}]^{6-}$ state on a given site, so the term with chemical potential μ allows to account for the charge density constraint, $nN = \langle \sum_i S_{zi} \rangle = const.$ Operators P_+^{ν} in (3) create holes with the spin projection ν and change the states $|00; \frac{1}{2}, -\nu\rangle$ into the states $|11;00\rangle$. Likewise, operators N_+^{ν} also create holes with the spin projection ν , but they transform the states $|1, -1;00\rangle$ into $|00; \frac{1}{2}\nu\rangle$. Operators S_+^2 in (4) creates the singlet hole pairs on the $[{\rm CuO_4}]^{7-}$ centers, and, obviously, the following relations for the one-hole and two-hole creation operators are fulfilled: $S_+^2 = P_+^{\nu} N_+^{-\nu}$. The explicit form of matrices for operators in equations (2–5) in the basis of states $|SM; s\mu\rangle$ is given in Appendix.

Using the quasi-classical approximation, we write the on-site wave function as follows

$$|\Psi\rangle = c_1 |11;00\rangle + c_{\uparrow} |10; \frac{1}{2} \frac{1}{2} \rangle + c_{\downarrow} |10; \frac{1}{2}, -\frac{1}{2} \rangle + c_{-1} |1, -1; 00\rangle,$$
 (6)

where the complex coefficients can be written in the following form:

$$c_k = r_k e^{i\phi_k}, \qquad \sum_k r_k^2 = 1,$$
 (7)

with phases $\phi_k \in [0, 2\pi]$, and we parametrize magnitudes r_k by angles $\theta, \varphi, \psi \in [0, \frac{\pi}{2}]$:

$$r_1 = \cos\theta\cos\varphi, \tag{8}$$

$$r_{\uparrow} = \sin \theta \cos \psi, \tag{9}$$

$$r_{\downarrow} = \sin \theta \sin \psi, \tag{10}$$

$$r_{-1} = \cos\theta\sin\varphi. \tag{11}$$

The average values for all operators in the Hamiltonian (1) are given in Appendix.

The energy for a model (1) in the quasi-classical approximation

$$E = \left\langle \prod_{i} \Psi_{i} \middle| \mathcal{H} \middle| \prod_{i} \Psi_{i} \right\rangle \tag{12}$$

have the following form:

$$\begin{split} E &= \sum_{i} \left(\Delta - \mu \cos 2\varphi_{i} \right) \cos^{2}\theta_{i} + V \sum_{\langle ij \rangle} \cos^{2}\theta_{i} \cos 2\varphi_{i} \cos^{2}\theta_{j} \cos 2\varphi_{j} - \\ &- \frac{t_{p}}{2} \sum_{\langle ij \rangle} \sin 2\theta_{i} \cos \varphi_{i} \sin 2\theta_{j} \cos \varphi_{j} \left(\cos \psi_{i} \cos \psi_{j} \cos \left(\phi_{1i} - \phi_{\uparrow i} - \phi_{1j} + \phi_{\uparrow j} \right) + \\ &+ \sin \psi_{i} \sin \psi_{j} \cos \left(\phi_{1i} - \phi_{\downarrow i} - \phi_{1j} + \phi_{\downarrow j} \right) \right) - \\ &- \frac{t_{n}}{2} \sum_{\langle ij \rangle} \sin 2\theta_{i} \sin \varphi_{i} \sin 2\theta_{j} \sin \varphi_{j} \left(\cos \psi_{i} \cos \psi_{j} \cos \left(\phi_{-1i} - \phi_{\uparrow i} - \phi_{-1j} + \phi_{\uparrow j} \right) + \\ &+ \sin \psi_{i} \sin \psi_{j} \cos \left(\phi_{-1i} - \phi_{\downarrow i} - \phi_{-1j} + \phi_{\downarrow j} \right) \right) - \\ &- \frac{t_{pn}}{4} \sum_{\langle ij \rangle} \sin 2\theta_{i} \sin 2\theta_{j} \left[\cos \varphi_{i} \sin \varphi_{j} \left(\sin \psi_{i} \cos \psi_{j} \cos \left(\phi_{1i} - \phi_{\downarrow i} + \phi_{-1j} - \phi_{\uparrow j} \right) + \right. \\ &+ \cos \psi_{i} \sin \psi_{j} \cos \left(\phi_{1i} - \phi_{\uparrow i} + \phi_{-1j} - \phi_{\downarrow j} \right) \right) + \\ &+ \sin \varphi_{i} \cos \varphi_{j} \left(\sin \psi_{i} \cos \psi_{j} \cos \left(\phi_{-1i} - \phi_{\downarrow i} + \phi_{1j} - \phi_{\uparrow j} \right) + \right. \\ &+ \cos \psi_{i} \sin \psi_{j} \cos \left(\phi_{-1i} - \phi_{\uparrow i} + \phi_{1j} - \phi_{\downarrow j} \right) \right) \right] - \\ &- \frac{t_{b}}{2} \sum_{\langle ij \rangle} \cos^{2}\theta_{i} \sin 2\varphi_{i} \cos^{2}\theta_{j} \sin 2\varphi_{j} \cos \left(\phi_{-1i} - \phi_{1i} - \phi_{-1j} + \phi_{1j} \right) + \\ &+ Js^{2} \sum_{\langle ij \rangle} \sin^{2}\theta_{i} \sin^{2}\theta_{j} \left(\sin 2\psi_{i} \sin 2\psi_{j} \cos \left(\phi_{\uparrow i} - \phi_{\uparrow i} + \phi_{\downarrow j} \right) + \cos 2\psi_{i} \cos 2\psi_{j} \right). \end{split}$$

3. State selection algorithm

The magnitudes of coefficients r_k in Eq. (7) correspond to points in the octant of the 4-dimensional unit sphere. In the Metropolis algorithm, randomly generated states should form a uniform distribution in the phase space. For the parametrization (8–11), the solid angle element is $d\Omega = \cos\theta \sin\theta \,d\theta \,d\varphi \,d\psi$, thus, the state selection algorithm should consist of generation of uniformly distributed phases $\phi_k \in [0, 2\pi]$, uniformly distributed angle variables $\varphi, \psi \in [0, \pi/2]$, and uniformly distributed value $m = \cos^2\theta \in [0, 1]$, where $\theta \in [0, \pi/2]$. In this case, the MC simulation of model (13) involves using the chemical potential μ as external fixed parameter and the subsequent recalculation of the results in the variables charge density, n, and temperature, T.

To study the features of the parametrization (7–11) we can find the on-site charge density distribution which is generated by the state selection algorithm formulated above. For the on-site charge density, we obtain the following expression in terms of uniformly distributed variables φ and m:

$$n = r_1^2 - r_{-1}^2 = m\cos 2\varphi. (14)$$

The domains D(n) where $m \cos 2\varphi < n$ are shown in Fig. 1(a). Integrating over domain D(n), we find the on-site charge distribution function F(n)

$$F(n) = \frac{2}{\pi} \int_{D(n)} dm \, d\varphi = -\frac{1}{\pi} \arccos n + \frac{n}{\pi} \ln \frac{1 + \sqrt{1 - n^2}}{|n|},\tag{15}$$

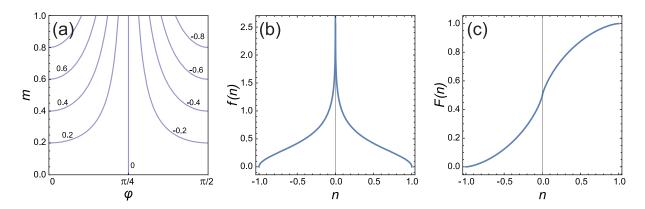


Figure 1. (a) The constant value lines for the on-site charge density n defined by Eq. (14); (b) the probability density function f(n); (c) the probability distribution function F(n).

and the corresponding probability density function f(n)

$$f(n) = \frac{1}{\pi} \ln \frac{1 + \sqrt{1 - n^2}}{|n|}.$$
 (16)

These functions are shown in Fig 1(b,c). As a specific feature of the parametrization (7–11), the probability density f(n) has a logarithmic singularity at n = 0.

One of the phase states in model (1) is the charge ordering. In this case, the function $n(\mu)$ has a typical step-like feature, when a small change in μ causes a large jump in n, from n_1 to n_2 , so, taking into account the statistical nature of the Monte Carlo method, it is difficult to obtain trustworthy simulation results for the range (n_1, n_2) . Further, we will consider an algorithm where the lattice state changes simultaneously on a pair of sites, but the total charge of the pair is conserved. This ensures the conservation of the total charge of the system during the simulation and allows us to study in detail the phase states of the system for all n.

If the states of a pair of sites 1 and 2 generated independently, the probability density to have the charge of the pair $2n = n_1 + n_2$ for a given charge n_1 at the site 1 is

$$f_1(n_1; 2n) = \frac{f(n_1)f(2n - n_1)}{\Phi(2n)} \tag{17}$$

where

$$\Phi(2n) = \int_{n_{1,min}}^{n_{1,max}} f(x)f(2n-x) dx,$$
(18)

and the function f(n) is defined by Eq. (16). The minimal and maximal values of n_1 at given 2n are

$$n_{1,min}(2n) = -1 + n + |n|, \qquad n_{1,max}(2n) = 1 + n - |n|.$$
 (19)

The cumulative distribution function $F_1(n_1; 2n)$ of the charge n_1 at the site 1 for the fixed pair charge 2n has the following form:

$$F_1(n_1; 2n) = \int_{n_{1,min}}^{n_1} f_1(x; 2n) \, dx. \tag{20}$$

The normalized probability density function $f_1(t;2n) = \Delta n_1 f_1(\Delta n_1 t + n_{1,min};2n)$, where $\Delta n_1 = n_{1,max} - n_{1,min}$, and cumulative distribution function $F_1(t;2n)$ are shown in Fig. 2. The

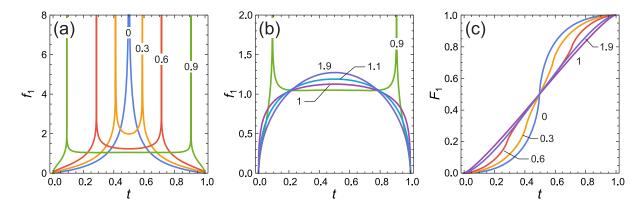


Figure 2. The normalized probability density function $f_1(t; 2n)$ for values of the pair charge (a) 2|n| = 0.0, 0.3, 0.6, 0.9; (b) 2|n| = 0.9, 1.0, 1.1, 1.9; (c) the cumulative distribution function $F_1(t; 2n)$ for 2|n| = 0.0, 0.3, 0.6, 1.0, 1.9.

probability density function f_1 has logarithmic singularities if 2|n| < 1 as shown in Fig. 2(a), and the corresponding distribution function F_1 has vertical tangents at these points. If $1 \le 2|n| < 2$, the probability density function has no singularities, so the distribution function only slightly deviates from the case of uniform distribution.

The uniform distribution in a phase space entails the constant probability density function $f(\varphi, m) = 2/\pi$ in the domain $0 \le m \le 1$, $0 \le \varphi \le \frac{\pi}{2}$ shown in Fig. 1(a). Since one of the new variables must be n_1 , we choose them as (n_1, m) . The domain in variables (φ, m) is mapped onto the domain in variables (n_1, m) shown in Fig.3(a). The new density function $p(n_1, m)$ is defined from equations

$$p(n_1, m) dn_1 dm = \frac{2}{\pi} \left| \frac{\partial \varphi}{\partial n_1} \right| dn_1 dm = \frac{dn_1 dm}{\pi \sqrt{m^2 - n_1^2}}.$$
 (21)

This allows us to find the conditional density function,

$$p_2(m|n_1) = \frac{1}{\pi f(n_1)\sqrt{m^2 - n_1^2}},$$
(22)

and the conditional distribution function:

$$F_2(m|n_1) = \frac{\ln\left(m + \sqrt{m^2 - n_1^2}\right) - \ln|n_1|}{\ln\left(1 + \sqrt{1 - n_1^2}\right) - \ln|n_1|}, \quad |n_1| \le m \le 1.$$
(23)

Fig.3(b,c) show the normalized conditional density function $p_2(t|n_1) = a p_2(at + |n_1||n_1)$, $a = (1 - |n_1|)$, and corresponding conditional distribution function $F_2(t|n_1)$ for some values of n_1 . The most significant variations of these functions take place in the region of small values of the parameter n_1 , therefore, values decreasing on a logarithmic scale are considered. For the state selection algorithm, it is necessary so solve an equation $F_2(m|n_1) = \gamma$ at given n_1 , so small values of n_1 can potentially lead to large inaccuracies. Fortunately, the explicit solution of equation $F_2(m|n_1) = \gamma$ can be written:

$$m = \frac{1}{2} \left[|n_1|^{1-\gamma} \left(1 + \sqrt{1 - n_1^2} \right)^{\gamma} + |n_1|^{1+\gamma} \left(1 + \sqrt{1 - n_1^2} \right)^{-\gamma} \right].$$
 (24)

The state selection algorithm for the quasi-classical Monte Carlo simulation of the model (1) that conserves the total charge consists of the following steps:

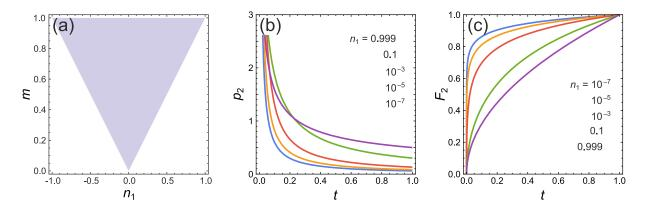


Figure 3. (a) The shaded area is the domain of functions in variables (n_1, m) ; (b) the conditional density function p_2 for given values of n_1 ; (c) the conditional distribution function F_2 for given values of n_1 .

- (i) calculation of the total charge $2n = n_{1,0} + n_{2,0}$ for the randomly selected pair of sites 1 and 2;
- (ii) calculation of the value n_1 from equation $F_1(n_1; 2n) = \gamma$, where $\gamma \in [0, 1]$ is the uniformly distributed random value, and the function $F_1(n_1; 2n)$ is defined by Eq. (20);
- (iii) calculation of the value $n_2 = 2n n_1$;
- (iv) calculation of values m_i , i = 1, 2, from equations $F_2(m_i|n_i) = \gamma_i$, where $\gamma \in [0, 1]$ is the uniformly distributed random value, the function $F_2(m|n)$ is defined by Eq. (23), and the explicit solution is given by Eq.(24);
- (v) calculation of φ_i i = 1, 2, from equations $\cos(2\varphi_i) = n_i/m_i$;
- (vi) calculation of θ_i , i = 1, 2, from equations $\cos^2 \theta_i = m_i$;
- (vii) generation of uniformly distributed random values $\phi_k^{(i)} \in [0, 2\pi], i = 1, 2, k = +1, -1, \uparrow, \downarrow,$ and $\psi_i \in [0, \frac{\pi}{2}], i = 1, 2.$

This allows us to find new states on the selected pair of sites using Eq. (6).

4. Results

In MC simulation, we calculated the structure factors

$$F_{\mathbf{q}}(A,B) = \frac{1}{N^2} \sum_{lm} e^{i\mathbf{q} \cdot (\mathbf{r}_l - \mathbf{r}_m)} \langle A_l B_m \rangle, \qquad (25)$$

where A_l and B_m are the on-site operators and the summation is performed over all sites of the square lattice. To determine the type of ordering, we monitored the following structure factors:

- $F_{(\pi,\pi)}(\boldsymbol{\sigma},\boldsymbol{\sigma})$ for antiferromagnetic (AFM) order,
- $F_{(\pi,\pi)}(S_z, S_z)$ for the charge order (CO),
- $F_{(0,0)}(S_+^2, S_-^2)$ for the superconducting order (SC),
- $F_{(0,0)}(P^+, P)$ for the "metal" phase (M).

Acknowledgments

The research was supported by UrFU Development Program "Priority-2030".

Appendix

The matrices of pseudospin operators on a given site in the basis $\{ |11;00\rangle, |10; \frac{1}{2}, \frac{1}{2}\rangle, |10; \frac{1}{2}, -\frac{1}{2}\rangle, |1, -1; 00\rangle \}$ have the following form:

$$\sigma_z = \begin{pmatrix} 0 & 0 & 0 & 0 \\ 0 & 1 & 0 & 0 \\ 0 & 0 & -1 & 0 \\ 0 & 0 & 0 & 0 \end{pmatrix}, \quad \sigma_x = \begin{pmatrix} 0 & 0 & 0 & 0 \\ 0 & 0 & 1 & 0 \\ 0 & 1 & 0 & 0 \\ 0 & 0 & 0 & 0 \end{pmatrix}, \quad \sigma_y = \begin{pmatrix} 0 & 0 & 0 & 0 \\ 0 & 0 & -i & 0 \\ 0 & i & 0 & 0 \\ 0 & 0 & 0 & 0 \end{pmatrix}.$$
(29)

Using equations (6–11), we can write average values $\langle A \rangle = \langle \Psi | A | \Psi \rangle$ for all operators in the Hamiltonian (1) on a given site:

$$\langle S_z \rangle = \cos^2 \theta \cos 2\varphi, \tag{30}$$

$$\langle S_z^2 \rangle = \cos^2 \theta, \tag{31}$$

$$\langle S_{+}^{2} \rangle = \frac{1}{2} e^{-i(\phi_{1} - \phi_{-1})} \cos^{2} \theta \sin 2\varphi, \qquad \langle S_{-}^{2} \rangle = \langle S_{+}^{2} \rangle^{*},$$
 (32)

$$\langle P_{+}^{\uparrow} \rangle = \frac{1}{2} e^{i(\phi_{\downarrow} - \phi_{1})} \sin 2\theta \sin \psi \cos \varphi, \qquad \langle P_{-}^{\uparrow} \rangle = \langle P_{+}^{\uparrow} \rangle^{*},$$
 (33)

$$\langle P_{+}^{\downarrow} \rangle = \frac{1}{2} e^{i(\phi_{\uparrow} - \phi_{1})} \sin 2\theta \cos \psi \cos \varphi, \qquad \langle P_{-}^{\downarrow} \rangle = \langle P_{+}^{\downarrow} \rangle^{*},$$
 (34)

$$\langle N_{+}^{\uparrow} \rangle = \frac{1}{2} e^{-i(\phi_{\uparrow} - \phi_{-1})} \sin 2\theta \cos \psi \sin \varphi, \qquad \langle N_{-}^{\uparrow} \rangle = \langle N_{+}^{\uparrow} \rangle^{*},$$
 (35)

$$\langle N_{+}^{\downarrow} \rangle = \frac{1}{2} e^{-i(\phi_{\downarrow} - \phi_{-1})} \sin 2\theta \sin \psi \sin \varphi, \qquad \langle N_{-}^{\downarrow} \rangle = \langle N_{+}^{\downarrow} \rangle^{*},$$
 (36)

$$\langle \sigma_x \rangle = \sin^2 \theta \sin 2\psi \cos (\phi_{\downarrow} - \phi_{\uparrow}),$$
 (37)

$$\langle \sigma_y \rangle = \sin^2 \theta \sin 2\psi \sin (\phi_{\downarrow} - \phi_{\uparrow}),$$
 (38)

$$\langle \sigma_z \rangle = \sin^2 \theta \cos 2\psi. \tag{39}$$

References

[1] Božović I, He X, Wu J and Bollinger A T 2016 Nature 536 309–311

- [2] Božović I, Wu J, He X and Bollinger A 2019 Physica C: Superconductivity and its Applications 558 30–37
- [3] Fradkin E and Kivelson S A 2012 Nature Physics 8 864–866
- [4] Moskvin A S and Panov Y D 2019 Journal of Superconductivity and Novel Magnetism 32 61–84
- [5] Moskvin A S 2011 Physical Review B 84 075116
- [6] Moskvin A S 2013 Journal of Physics: Condensed Matter 25 085601
- [7] Mallett B P P, Wolf T, Gilioli E, Licci F, Williams G V M, Kaiser A B, Ashcroft N W, Suresh N and Tallon J L 2013 *Physical Review Letters* **111** 237001
- [8] Moskvin A S and Panov Y D 2019 Physics of the Solid State 61 1553–1558
- [9] Castellani C, Castro C D, Feinberg D and Ranninger J 1979 Physical Review Letters 43 1957–1960
- [10] Rice T M and Sneddon L 1981 Physical Review Letters 47 689–692
- [11] Löw U, Emery V J, Fabricius K and Kivelson S A 1994 Physical Review Letters **72** 1918–1921
- [12] Panov Y, Ulitko V, Budrin K, Chikov A and Moskvin A 2019 Journal of Magnetism and Magnetic Materials 477 162–166
- [13] Yasinskaya D N, Ulitko V A and Panov Y D 2020 Physics of the Solid State 62 1713–1718
- [14] Cannas S A and Stariolo D A 2019 Physical Review E 99 042137
- [15] Frantz G L K, Schmidt M and Zimmer F M 2021 Physical Review E 103 032125